Extended optical model for fission

M. Sin,[1,*] R. Capote,[2,†] M. W. Herman,[3] and A. Trkov[2]
[1]*University of Bucharest, Faculty of Physics, Bucharest-Magurele, Romania*
[2]*NAPC–Nuclear Data Section, International Atomic Energy Agency, A-1400 Vienna, Austria*
[3]*National Nuclear Data Center, Brookhaven National Laboratory, New York, USA*
(Received 10 December 2015; published 7 March 2016)

A comprehensive formalism to calculate fission cross sections based on the extension of the optical model for fission is presented. It can be used for description of nuclear reactions on actinides featuring multi-humped fission barriers with partial absorption in the wells and direct transmission through discrete and continuum fission channels. The formalism describes the gross fluctuations observed in the fission probability due to vibrational resonances, and can be easily implemented in existing statistical reaction model codes. The extended optical model for fission is applied for neutron induced fission cross-section calculations on ^{234,235,238}U and ^{239}Pu targets. A triple-humped fission barrier is used for ^{234,235}U(n,f), while a double-humped fission barrier is used for ^{238}U(n,f) and ^{239}Pu(n,f) reactions as predicted by theoretical barrier calculations. The impact of partial damping of class-II/III states, and of direct transmission through discrete and continuum fission channels, is shown to be critical for a proper description of the measured fission cross sections for ^{234,235,238}U(n,f) reactions. The ^{239}Pu(n,f) reaction can be calculated in the complete damping approximation. Calculated cross sections for ^{235,238}U(n,f) and ^{239}Pu(n,f) reactions agree within 3% with the corresponding cross sections derived within the Neutron Standards least-squares fit of available experimental data. The extended optical model for fission can be used for both theoretical fission studies and nuclear data evaluation.

DOI: 10.1103/PhysRevC.93.034605

I. INTRODUCTION

Recently, the Nuclear Energy Agency started a new international collaboration called CIELO (Collaborative International Evaluated Library Organisation) with the main goal to improve our understanding of neutron reactions on key isotopes that are important in nuclear applications, especially in the area of criticality safety and reactors [1,2]. Among the six nuclei selected for the pilot CIELO project, a prominent role is played by the three major actinides, ^{235,238}U and ^{239}Pu, for which fission is the single most important reaction to be studied.

Fission cross sections for neutron induced reactions on major actinides represent the largest amount of experimental data compiled in the EXFOR database [3]. The abundance of high-quality measurements allowed the least-squares evaluation of fission cross sections of major actinides for fast neutron induced fission to be based exclusively on the available experimental data. The latest least-squares evaluation was undertaken within the Neutron Standards project [4,5] and resulted in evaluated fission cross sections of major actinides with tight uncertainties. However, a consistent evaluation of all reaction channels in the whole energy range of interest studied in the CIELO project [2,6] requires reaction models that describe the evaluated fission cross sections (Neutron Standards) within the evaluated uncertainty. Such description allows proper modeling not only of the fission channel but also of the main competing channels: neutron capture, elastic and inelastic scattering, and multiple neutron emission [7,8].

In spite of great efforts devoted to the study of the fission phenomena since its discovery in 1938 [9,10], our capabilities to predict fission cross sections for fast neutron induced reactions remain limited (e.g., see Ref. [11] and references therein). An extension of the R-matrix theory to the fission deformation variable as outlined by Bjørnholm and Lynn [12] has been recently suggested by Bouland *et al.* [13]. The new model has been successfully applied to study neutron induced fission of double-humped barrier plutonium isotopes, and some predictive capability was achieved [13]. Further theoretical studies are needed to meet the needs of nuclear data evaluation of many actinide nuclei, as well as for a better understanding of the observed fission cross sections in the fast neutron range.

One of most successful approaches used to calculate the fission cross section is the optical model for fission, which has a history of more than four decades. It was realized by Lynn in 1966 [14] that the treatment of the fission process can be extended to consider other degrees of freedom by treating excitation of the latter as simple absorption out of the fission mode. A similar assumption is the basis of the highly successful nuclear optical model describing nuclear particle scattering [15]. Soon after the discovery of the secondary minimum in the fission barrier by Strutinsky [16,17] it was noted that the sub-barrier resonances in the fission probability of different actinides, identified as vibrational excitations in the second well (class-II states), were broader than the expected penetrability of the two peaks [18–20]. This was similarly explained by the coupling between the fission mode and the internal degrees of freedom in the second well; in other words by the damping of the class-II vibrational strength [20–22]. The damping was phenomenologically simulated by adding to the real part of the deformation potential an imaginary term in the region of the second well to absorb out flux from the fission mode and to redistribute it into internal excitations

*mihaela.sin@g.unibuc.ro
†r.capotenoy@iaea.org

[20–24]. The damping is expected to increase dramatically when the vibrational energy of the fission mode is above the fission barrier, because the effective excitation energy of the fission mode rises to that of the compound nucleus [20]. The optical model for fission is applicable starting at those energies for which all the excited states acquire fission widths. Approximately at the same limit the statistical hypothesis regarding the nuclear resonances becomes valid. Initially, the optical model for fission was used mostly for calculating the fission probability in direct reactions with incident charged particles in a narrow range of incident particle energies [25–28].

Fast neutron induced fission cross sections for nuclear data evaluation were calculated for a long time using the classical expression for the penetrability through double-humped barriers corresponding to the complete (full) damping limit; i.e., all the incoming flux is absorbed in the secondary well, and later re-emitted into the fission channel. In this way the fission competition was approximately considered above the barrier. However, within the full damping limit, the sub-barrier vibrational resonance structure in the fission cross sections of fertile nuclei could not be described, and experimental fission data at low incident energies were usually overestimated. A poor description of the fission channel resulted in correspondingly poor calculation of cross sections of competing channels. The poor description of channels competing with fission was reflected in the large discrepancies observed among evaluated data for reactions with poor experimental data, e.g., for neutron capture of fissile actinides and especially for neutron inelastic scattering [29].

To address these problems, the concept of the optical model for fission was included in the statistical model. To the best of our knowledge STATIS [30] was the first statistical reaction code in which the optical model for fission was implemented. However, the descriptive power of the optical model for fission was fully exploited only after it was implemented in the EMPIRE code [31]. Since then, it has been continuously updated by incorporating fundamental features of the fission process confirmed or revealed by the experimental data and further theoretical studies. A significant step forward in the description of measured fission cross sections was the use of transmission coefficients through triple-humped barrier with absorption in the secondary well [32,33]. This version was used for the evaluation of neutron reaction data on ^{232}Th and ^{231,233}Pa [34] targets, which were later adopted by the U.S. national data library [35]. The optical model for fission to treat more than two fission barriers was simplified, and at the same time generalized, when a recursive method to calculate transmission through n-humped barriers with absorption in all wells was suggested in Ref. [36]. Because the model was designed to consider only the damping of the discrete vibrational states accommodated by the minima of the fission barrier (wells), an approximate method to consider the partial absorption through the fission continuum channels was added later [37].

This paper provides a complete and comprehensive description of an extended formalism based on the optical model for fission for cross-section calculations within the statistical model in Sec. II. Fission cross-section calculations for four representative test cases are undertaken for ^{234,235,238}U(n,f) and ^{239}Pu(n,f) reactions using the updated optical model for fission described in Sec. III. Finally, conclusions are given.

II. OPTICAL MODEL FOR FISSION

The transmission through a multi-humped fission barrier depends on the degree of damping of the vibrational states in the potential minima. The two extreme cases for a transmission through a real fission potential with N_h humps are

(1) *zero damping (no absorption)* valid at low excitation energies where fission occurs directly, without involving other internal degrees of freedom; in this case the fission coefficient is equal to the direct transmission coefficient $T_f = T_{d_{(0)}}$ representing the barrier transmission probability [defined generically by Eq. (8)];

(2) *complete damping (full absorption)* valid for excitation energies close to or above the top of the highest barrier, where all transmitted flux is absorbed in the wells, and later re-emitted into the fission channel; in this case the humps can be considered decoupled (independent) and the fission coefficient becomes

$$T_f = \left[\sum_{h=1}^{N_h} \frac{1}{T_h}\right]^{-1}, \tag{1}$$

where T_h represents the penetrability through the individual hump h.

A complex fission potential is used in the optical model for fission to describe the partial damping of the class-II/III vibrational states in the wells, allowing a smooth transition between the two extreme situations described above. Within this model, fission occurs by direct transmission across the barrier(s) and by re-emission into the fission channel after absorption into the isomeric well(s). The fission transmission coefficients associated to these two mechanisms are the direct transmission coefficient (T_d) and the indirect (T_i) one, respectively, the sum of their contributions representing the total fission coefficient $T_f \equiv T_d + T_i$.

A recursive method to calculate the fission transmission coefficients through a barrier with N_h humps and N_w wells was proposed in Ref. [36]. Using the notation appropriate for recursive derivation, the general expression for the fission coefficient is

$$T_f = T_d^{(1,N_h)} + R\sum_{w=2}^{N_w} T_i^{(w)}, \tag{2}$$

where $T_d^{(1,N_h)}$ represents the direct transmission coefficient through all humps (starting with hump 1 and ending with hump N_h), $T_i^{(w)}$ stands for the indirect transmission coefficient associated with the well w, and R is a normalization factor [36].[1]

[1]Direct $T_d^{(1,N_h)}$ and indirect $T_i^{(w)}$ transmission coefficients were denoted as $T_d(1,N_h)$ and $T_i(w)$ respectively in Ref. [36].

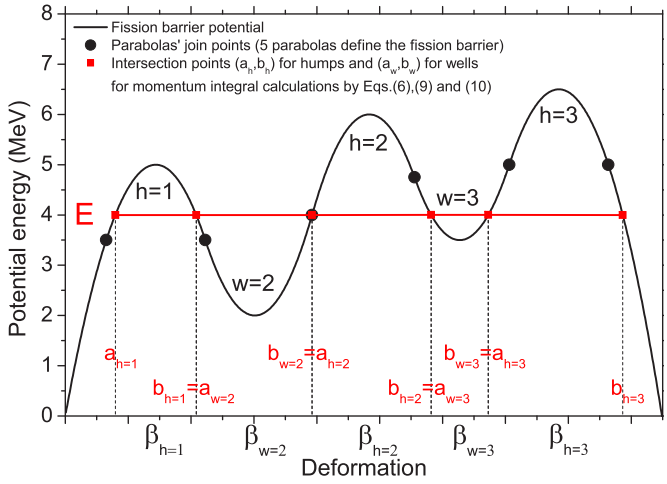

FIG. 1. A triple-humped fission barrier and associated parameters.

A. Transmission coefficients

The transmission calculation requires a definition of the barrier. The barriers can be defined numerically or analytically. For this paper we chose for simplicity (without any loss of generality) a classical barrier parametrization as a function of the quadrupole deformation β by smoothly joined parabolas as shown in Fig. 1:

$$E_h^{\rm def}(\beta) = V_h - \tfrac{1}{2}\mu(\hbar\omega_h)^2(\beta-\beta_h)^2, \quad h=[1,N_h],$$
$$E_w^{\rm def}(\beta) = V_w + \tfrac{1}{2}\mu(\hbar\omega_w)^2(\beta-\beta_w)^2, \quad w=[2,N_w], \tag{3}$$

where h is the barrier index that runs from 1 to N_h; w is the well index that runs from 2 to N_w because the first well, corresponding to equilibrium deformation, is not included in the parametrization (as the model assumes the full damping of the class-I vibrational states).

The energies V_h (V_w) correspond to the maxima (minima) of the potential in the hump (well) region, β_h (β_w) are the corresponding deformations (abscissae), the harmonic oscillator frequencies $\hbar\omega_h$ ($\hbar\omega_w$) define the curvature of each parabola for barriers (h) and wells (w), and μ is the inertial mass parameter, assumed to be independent of the deformation β. The numerical integration method used below to calculate the penetrability makes it easy to remove the latter approximation if desired. The fission barrier just defined would correspond to the lowest excitation state of the nucleus along the fission path; i.e., it is the so-called fundamental barrier. There are additional barriers built on both discrete and continuum transition states above it. The same method used to calculate the fission cross section through the fundamental barrier can be used for those barriers built on transition states, as will be shown in Sec. II B.

The damping of the class-II/III vibrational states within wells is simulated by introducing negative imaginary potentials, iW_w, in the corresponding deformation ranges, which causes absorption of the incoming flux in these wells [14,20,22,23,26]. The imaginary potential strengths W_w are assumed to be quadratic functions of the deformation β, like the real part, but the excitation energy dependence is also included in the potential strength [factor $\alpha_w(E)$]:

$$W_w(\beta) = -\alpha_w(E)\big[E - E_w^{\rm def}(\beta)\big], \quad w=[2,N_w], \tag{4}$$

where E is the excitation energy of the fissioning nucleus. The factors $\alpha_w(E)$ help control the strength of the imaginary parts of the fission potential. These factors are chosen to allow the fit of the resonances in sub-barrier fission cross section and to guarantee a proper asymptotic behavior of transmission coefficients at higher excitation energies.

1. Single-humped barrier

The transmission coefficient T_h is expressed in the first-order Jeffreys-Wentzel-Kramers-Brillouin (JWKB) approximation in term of the momentum integral K_h for the hump [38,39]:

$$T_h = \frac{1}{1+\exp(2K_h)}, \tag{5}$$

with the momentum integral given by

$$K_h = \pm\left|\int_{a_h}^{b_h}\left[\frac{2\mu}{\hbar^2}\big(E - E_h^{\rm def}(\beta)\big)\right]^{1/2} d\beta\right|, \tag{6}$$

where a_h,b_h stand for the intercepts (see Fig. 1), the plus sign is taken when the excitation energy is lower than the hump under consideration, and the minus when it is higher. In the latter case, the intercepts are complex conjugate ($b_h = a_h^*$), and the JWKB approximation is valid when their imaginary parts are small, i.e., for energies slightly higher than the hump. For a single parabolic barrier with height V and curvature $\hbar\omega$, Eqs. (5) and (6) yield the well-known Hill-Wheeler transmission coefficient [12,40], which is an exact result:

$$T_{HW} = \frac{1}{1+\exp\left[\frac{2\pi}{\hbar\omega}(V-E)\right]}. \tag{7}$$

2. Double-humped barrier

For a real double-humped barrier the direct transmission coefficient calculated in JWKB approximation reads [32,41,42]

$$T_{d_{(0)}}^{(1,2)} = \frac{T_1 T_2}{1+2A^{1/2}\cos(2\nu_2)+A}, \tag{8}$$

where ν_2 represents the momentum integral for the secondary well; $A=(1-T_1)(1-T_2)$, with T_1, T_2 being the transmission coefficients through humps 1 and 2 respectively, given by Eq. (5). The momentum integral depending on the real part of the potential for an intermediate well w is approximated as

$$\nu_w = \int_{a_w}^{b_w}\left[\frac{2\mu}{\hbar^2}\big(E - E_w^{\rm def}(\beta)\big)\right]^{1/2} d\beta, \qquad w=2. \tag{9}$$

where a_w,b_w stand for the intercepts with the potential well (see Fig. 1).

When an imaginary potential $W_w(\beta)$ in the deformation range corresponding to the secondary well ($w=2$) given by Eq. (4) is added to the real barrier defined by Eq. (3), then part of the initial flux is transmitted directly, the rest is being absorbed in the secondary well. The expressions for the direct transmission coefficient and for the absorption coefficient are

taken from Bhandari [32,41]. The definition of the direct transmission coefficient through a double-humped barrier in the presence of absorption is a generalization of Eq. (8). It is obtained by adding the real momentum integral ν_2 to the contribution δ_2 corresponding to the imaginary potential in the second well as shown by Bhandari [32,41]:

$$\delta_w = -\left(\frac{\mu}{2\hbar^2}\right)^{1/2} \int_{a_w}^{b_w} \frac{W_w(\beta)}{\left[E - E_w^{\rm def}(\beta)\right]^{1/2}} d\beta, \quad w = 2. \tag{10}$$

$$T_d^{(1,2)} = \frac{T_1 T_2}{e^{2\delta_2} + 2A^{1/2}\cos(2\nu_2) + Ae^{-2\delta_2}}, \tag{11}$$

where $A = (1 - T_1)(1 - T_2)$ as before.

The absorption coefficient associated to the shape transition from the equilibrium deformation ($w = 1$) to the superdeformed isomeric well ($w' = 2$) reads

$$T_a^{(1,2)} = T_d^{(1,2)}\left[\frac{e^{2\delta_2} - [1 - T_2]e^{-2\delta_2} - T_2}{T_2}\right]. \tag{12}$$

If the imaginary potential is zero, then the phase $\delta_2 \equiv 0$, and $T_a^{(1,2)} \to 0$ as expected. The fraction of the incoming flux absorbed in the secondary (isomeric) well can (i) be re-emitted in the fission channel (indirect prompt fission), (ii) return back to a class I state, or (iii) undergo γ transition to the isomeric state. The isomeric state, in turn, can decay by delayed (isomeric) fission or by shape transition to class-I states. The general expression of the fission coefficient T_f given in Eq. (2) becomes for a double-humped barrier

$$T_f = T_d^{(1,2)} + RT_i^{(2)}, \qquad R \equiv 1. \tag{13}$$

Neglecting the delayed (isomeric) fission, the indirect transmission coefficient representing emission in the fission channel after absorption in the isomeric well is defined as

$$T_i^{(2)} = T_a^{(1,2)} \frac{T_2}{\sum T(2)}, \tag{14}$$

where the denominator stands for the sum of the transmission coefficients for the competing channels specific to the second well,

$$\sum T(2) = T_1 + T_2 + T_\gamma^{(2)}. \tag{15}$$

The γ-transition coefficient to the isomeric state $T_\gamma(2)$ (within the secondary well) might be important, becoming comparable to the transmissions through the inner and outer humps, when the compound nucleus is populated in states with small excitation energies with respect to the bottom of the isomeric well. This could happen in photofission, after direct transfer reactions, and in special cases of neutron induced fission. To account for the delayed fission, the term $T_a^{(1,2)}T_\gamma(2)R_{\rm iso}/\sum T(2)$, has to be added to the indirect fission coefficient $T_i^{(2)}$ defined by Eq. (14). The factor $R_{\rm iso}$ represents the ratio of the decay widths for fission and for the shape transition back to the equilibrium deformation of the isomeric state. The isomeric fission is neglected in this work.

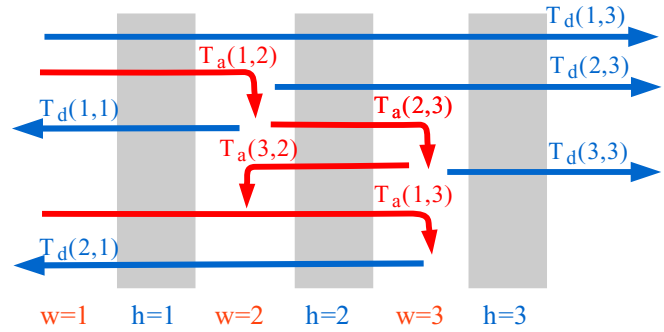

FIG. 2. Schematic representation of the transmission flux for a triple-humped fission barrier. w (h) values indicated below the figure represent the well (barrier) index. The coefficients $T_a(w,w')$ that represents the absorption in a well w of the flux coming from the well w' are shown as bent arrows (in red), the coefficients $T_d(h,h')$ that represent the transmission through the humps h and h' are shown as straight arrows (in blue), and the coefficients $T_d(h,h) \equiv T_h$ represent the transmission through a single hump h. Arrows pointing to the right (left) represent the forward (backward) directions. Isomeric gamma decay (within the wells) and delayed (isomeric) fission are not included in the scheme.

3. *Triple-humped barrier*

For barriers with more than two humps, the transmission coefficients can be calculated recursively, using as a reference the double-humped equations given in the previous section as shown in Ref. [36]. It was demonstrated in Ref. [36] that the results of recursive calculation agree exactly with those independently obtained for transmission through real potentials by Martinelli *et al.* [43] and Bhandari [44,45], as well as with the transmission coefficients through a triple-humped barrier that consider absorption in the second well [33].

The direct and absorption transmission coefficients associated to a triple-humped fission barrier are represented in Fig. 2. The required forward ($h < h'$) and backward ($h > h'$) direct transmission coefficients $T_d^{(1,3)}$, $T_d^{(2,3)}$, and $T_d^{(2,1)}$, respectively, can be calculated with the general expression

$$T_d^{(h,h')} = \frac{T_h T_d^{(h+1,h')}}{e^{2\delta_w} + 2A^{1/2}\cos(2\nu_w) + Ae^{-2\delta_w}}, \qquad h \neq h', \tag{16}$$

where $A = (1 - T_h)(1 - T_d^{(h+1,h')})$, $T_d^{(h,h)} \equiv T_h$, the transmission coefficients T_h through one hump h are given by Eq. (5), and the required index combinations shown in Fig. 2 are

$h' = 2,3,$	$h = [1,h' - 1],$	$w = h + 1,$	forward transmission (1,2), (2,3), (1,3);
$h' = 1,$	$h = 2,$	$w = 2,$	backward transmission (2,1).

The forward absorption coefficients $T_a^{(1,2)}$, $T_a^{(1,3)}$, and $T_a^{(2,3)}$ between the wells w and w' ($w < w'$)

$$T_a^{(w,w')} = T_d^{(h,3)}\left[\frac{e^{2\delta_{w'}} - \left[1 - T_d^{(h',3)}\right]e^{-2\delta_{w'}} - T_d^{(h',3)}}{T_d^{(h',3)}}\right], \tag{17}$$

where $h = w$ and $h' = w'$.

The required backward absorption coefficient from the third to the second well reads

$$T_a^{(3,2)} = T_d^{(2,1)}\left[\frac{e^{2\delta_2} - [1 - T_1]e^{-2\delta_2} - T_1}{T_1}\right]. \tag{18}$$

The general expression of the fission coefficient given in Eq. (2) becomes in the case of a triple-humped barrier

$$T_f = T_d^{(1,3)} + R\left[T_i^{(2)} + T_i^{(3)}\right]. \tag{19}$$

The indirect transmission coefficients $T_i^{(w)}$ corresponding to the transmission through the outer humps after absorption in the second and third wells read

$$T_i^{(w)} = T_a^{(1,w)}\left[\frac{T_d^{(h,3)}}{\sum T(w)} + \frac{T_a^{(w,w')}}{\sum T(w)}\frac{T_d^{(h',3)}}{\sum T(w')}\right], \tag{20}$$

where $w = (2,3)$, $w' = (2,3)$, $w' \neq w$, and $h = w, h' = w'$, respectively. The normalization factor R takes into account the effect of the infinite number of shape transitions and guarantees the flux conservation. It can be calculated as given in Ref. [36]:

$$R = \left[1 - \frac{T_a^{(2,3)}}{\sum T(2)}\frac{T_a^{(3,2)}}{\sum T(3)}\right]^{-1}. \tag{21}$$

The sums of the transmission coefficients for the competing channels specific to the second and third wells are

$$\sum T(2) = T_1 + T_d^{(2,3)} + T_a^{(2,3)} + T_\gamma^{(2)}, \tag{22}$$

$$\sum T(3) = T_d^{(2,1)} + T_3 + T_a^{(3,2)} + T_\gamma^{(3)}. \tag{23}$$

B. Effective fission coefficients

The fission coefficients presented before correspond to transmission through only one barrier associated to a single fission path defined by the angular momentum J, parity π, and angular momentum projection on the nuclear symmetry axis K. However, the fission coefficients used in the statistical models correspond to the transmission through all barriers associated with the discrete transition states, and to the continuous spectrum of the transition states having the same quantum numbers $J\pi$; see Eq. (41). The calculation of effective fission coefficients is presented after a brief description of the barriers associated with the excited states of the nucleus along the fission path.

The discrete excited states are rotational levels built on vibrational or single-particle band heads characterized by a given set of quantum numbers $(K, J\pi)$. The excitation energies at the deformation corresponding to the hump h (or well w) of such a state are

$$E_i(KJ\pi) = V_i + \epsilon_i(K,\pi) + \frac{\hbar^2}{2\Im_i}[J(J+1) - K(K+1)], \quad i \text{ runs over all humps and wells}, \tag{24}$$

where V_i is the top of the barrier $i = h$ or the bottom of the well $i = w$, respectively; $\epsilon_i(K,\pi)$ are the rotational band-head energies of the transitional or class-II/class-III band with quantum numbers $K\pi$, and $\hbar^2/2\Im_i$ are the inertial parameters of the same band (the decoupling parameter for $K = 1/2$ bands was neglected). A parabolic barrier (or well) with height (depth) $E_h(J,K,\pi)$ ($E_w(J,K,\pi)$) and curvature $\hbar\omega_h$ ($\hbar\omega_w$) is associated with each transition or class-II/class-III state. Usually, these are free parameters and their values are extracted from systematics or are obtained from the fit of the experimental fission cross section. It should be noted that, for nonaxial shapes at the inner saddle, additional $2J + 1$ rotational levels for each J should be assumed. On the other hand, the rotational bands (e.g., with $K = 1/2, 3/2, 5/2, \ldots$) at the outer saddle do not have a parity, and an additional factor of 2 is assumed due to the mass asymmetry. This factor is taken into account at the level of transmission coefficients as described later.

The transitional state spectrum has a discrete component up to certain energies E_{ch}, above which it is continuous and described by the level density function $\rho_{f_h}(EJ\pi)$, accounting for collective enhancements specific to the nuclear shape asymmetry at each saddle point (see next section).

In principle, the excited states in the continuum for the equilibrium deformation (normal states) and above the saddle points (transitional states) should be described by the same type of level density function $\rho(EJ\pi)$, which can be defined numerically or analytically. The parameters of the level density functions, such as the shell corrections and their damping parameters, the pairing energy, or the asymptotic values of the a parameter, are strongly interrelated, and depend on their corresponding values for the equilibrium deformation. Therefore, it is difficult to provide a general prescription for their calculation. Another impediment is the lack of experimental information such as the cumulative number of low-lying levels and the mean level distance at the neutron separation energy usually used to constrain the density of the normal states. Potentially, we could do systematic Strutinsky type calculations to extract those parameters; this work is planned, but it is outside the scope of the present paper. We adopt RIPL recommendations [46,47] where available (e.g., shell corrections, pairing energy), replace the equilibrium deformation with the deformations corresponding to the wells and saddle points (e.g., moments of inertia), and deduce other parameters, such as the asymptotic value of the transition level density or the collective enhancement, from the fit of the experimental fission cross sections for a significant number of actinides. Another feature with an important impact on the transition state spectrum is the order of symmetry of the nuclear shape at saddles. This is taken into account by multiplying the level density with an enhancement factor $f_{\text{sym}}(h)$ associated with the nuclear shape symmetry at each saddle, as shown in Ref. [48].

For a single-humped barrier h, the transmission coefficient is the sum of two contributions corresponding to the discrete and continuous parts of the transition state spectrum,

$$T_h(EJ\pi) = T_{h,\mathrm{dis}}(EJ\pi) + T_{h,\mathrm{cont}}(EJ\pi),$$
$$T_h(EJ\pi) = \sum_{K\leqslant J} T_h(EKJ\pi) + \int_{E_{ch}}^{\infty} \frac{\rho_h(\varepsilon J\pi)d\varepsilon}{1+\exp\left[-\frac{2\pi}{\hbar\omega_h}(E-V_h-\varepsilon)\right]}, \quad (25)$$

where $T_h(EKJ\pi) \equiv T_d^{(h,h)} = T_h$ is given by Eq. (5) and $\rho_h(\varepsilon J\pi)$ is the level density at the saddle h, with ε representing the excitation energy with respect to the top of the hump. In the same way, the direct transmission coefficients through barriers h and h' and the absorption coefficients from well w to well w' considering the discrete and continuum spectrum are expressed as

$$T_{\mathrm{dir}}^{(h,h')}(EJ\pi) = T_{\mathrm{dir,dis}}^{(h,h')}(EJ\pi) + T_{\mathrm{dir,cont}}^{(h,h')}(EJ\pi), \quad (26)$$

$$T_{\mathrm{abs}}^{(w,w')}(EJ\pi) = T_{\mathrm{abs,dis}}^{(w,w')}(EJ\pi) + T_{\mathrm{abs,cont}}^{(w,w')}(EJ\pi). \quad (27)$$

1. Transmission through discrete barriers

The structure of the saddle transition states is very complex, and it is still difficult to predict it accurately. It depends on the odd-even-A type and on the asymmetries of the nuclear shape at saddle deformation. For consistency, enhancement factors $d_{\mathrm{sym}}^{(h)}$ equal to the same enhancement factors applied for the level density functions which describe the transition states in the continuum $f_{\mathrm{sym}}(h)$ should be applied to the discrete transition states. Obviously, due to the spin-parity selection rules, this method is not equivalent to taking into account properly the double degeneracy of the K bands at the outer saddle(s), but our tests indicated that the impact of this assumption on the calculated fission cross section is small.

In the present formalism we attempt to keep both the spirit of the optical model for fission and a manageable fission input, but to consider at the same time the partial lift of degeneracy associated to the nuclear shape asymmetry. Therefore, the symmetry enhancements are applied on the transmission coefficients and not on the discrete levels.

For the transmission coefficient through a single hump h, things are straightforward: the first term (transmission through discrete fission channels) in Eq. (25) is replaced with

$$T_{h,\mathrm{dis}}(EJ\pi) = \sum_{K\leqslant J} d_{\mathrm{sym}}^{(h)} T_h(EKJ\pi), \quad h=[1,N_h]. \quad (28)$$

The calculation of direct transmission coefficients through humps h and h' in the optical model for fission requires a full fission path along the deformation variable. That is why the enhancement applied to these coefficients $d_{\mathrm{sym}}^{\mathrm{min}}$ represents the minimum among the enhancements of the transition states at the humps crossed:

$$T_{\mathrm{dir,dis}}^{(h,h')}(EJ\pi) = \sum_{K\leqslant J} d_{\mathrm{sym}}^{\mathrm{min}} T_d^{(h,h')}(EKJ\pi), \quad (29)$$

where $T_d^{(h,h')}(EKJ\pi)$ are given by Eq. (16), and $d_{sym}^{min} = min(d_{sym}^{(h)}, d_{sym}^{(h')})$ for $h=[1,N_h]$, $h'=[1,N_h]$, $h\neq h'$.

For the indirect fission coefficients through the well(s), the way the sum rule applies depends on the assumptions concerning the preservation of the quantum number K in the isomeric well(s). In the description of fission cross sections, one can consider two extreme cases: the first case assumes that fission mainly proceeds through discrete transition states characterized by well-defined values of K and is known as "no K mixing" approximation; the second case considers that the excitation of internal degrees of freedom in the second well makes it possible for the nucleus to change its K value during the time the energy is bound in internal motions and this effect is referred to as "full K mixing." The effect of these approximations on the fission probability is very small, but they can affect significantly the angular correlations of the fission fragments [26]. The appropriate choice for the purpose of nuclear data evaluation is the "full K mixing" approximation, not only for physical reasons, but also because it can be applied at any excitation energy. Formally, "full K mixing" is described by adding the absorption from different transition states irrespective of the associated K value into a quantity preserving the spin and parity. The main consequence is that the absorption coefficient for a certain $J\pi$ that appears in Eq. (27) is

$$T_{\mathrm{abs,dis}}^{(w,w')}(EJ\pi) = \sum_{K\leqslant J} d_{\mathrm{sym}}^{(h)} T_a^{(w,w')}(EKJ\pi), \quad (30)$$

with $T_a^{(w,w')}(EKJ\pi)$ given by Eqs. (17) and (18).

2. Transmission through double-humped continuum barriers

In the case of double-humped barriers the contribution of the fission channels in the continuum increases with excitation energy, and it becomes significant only at those excitation energies for which the class-II vibrational states become completely damped. Formally, for these energies the strength of the imaginary potential is high enough to consider that the entire flux transmitted through the inner hump is absorbed in the second well as discussed, e.g., by Lynn [20]. Therefore, the direct transmission through the continuum for all barriers disappears:

$$T_{\mathrm{dir,cont}}^{(1,2)}(EJ\pi) = 0,$$
$$T_{\mathrm{abs,cont}}^{(1,2)}(EJ\pi) = \int_{E_{c1}}^{\infty} \frac{\rho_1(\varepsilon J\pi)d\varepsilon}{1+\exp\left[-\frac{2\pi}{\hbar\omega_1}(E-V_1-\varepsilon)\right]}. \quad (31)$$

There are cases when a simpler approach to calculate the fission coefficient may be used that does not involve information about the discrete (transitional and class-II) states or the imaginary potential, as discussed in Ref. [37]. Considering the case where the transitional state spectrum is exclusively continuous and applying the above Eq. (31), the fission coefficient that corresponds to the full damping limit defined by Eq. (1) is obtained. This might lead to an overestimation of the fission cross section at sub-barrier energies. To overcome this problem, still using a simplified approach, we developed an alternative method to consider the partial absorption appropriate for the fission channels described by the level densities at saddles. As the method does not involve an imaginary potential, we refer to it as a surrogate of the optical model for

fission [37]. In this model, the degree of damping is taken into account by defining the total fission coefficient as a weighted sum of the two extreme cases previously discussed: a direct transmission coefficient corresponding to the zero-damping limit, and an indirect coefficient corresponding to the full damping of the vibrational states in the well:

$$T_f(EJ\pi) = [1 - p_2(E)]T^{(1,2)}_{d_{(0)},\mathrm{cont}}(EJ\pi) + p_2(E)T^{(2)}_{i_{(f)},\mathrm{cont}}(EJ\pi). \quad (32)$$

The direct coefficient corresponding to the zero-damping limit $T^{(1,2)}_{d_{(0)},\mathrm{cont}}$ is given by Eq. (8), which defines transmission through a real potential averaged to avoid fluctuations [$\overline{\cos(2\nu_2)} \to 0$], and adapted for transmission in the continuum:

$$T^{(1,2)}_{d_{(0)},\mathrm{cont}}(EJ\pi) = \int_{E_c}^{\infty} \overline{T^{(1,2)}_{d_{(0)}}}(E-\varepsilon, J\pi)\rho_{\min}(\varepsilon J\pi)d\varepsilon, \quad (33)$$

where

$$\overline{T^{(1,2)}_{d_{(0)}}} = \frac{T_1 T_2}{1+A}, \quad (34)$$

with $A = (1-T_1)(1-T_2)$, and $\rho_{\min}(\varepsilon J\pi)$ is the minimum of the level density at corresponding saddle points that is supposed to control the direct transmission.

The indirect coefficient in the full damping limit $T^{(2)}_{i_{(f)},\mathrm{cont}}$ is defined by Eq. (14), which is equivalent to Eq. (1). For transmission in the continuum it reads

$$T^{(2)}_{i_{(f)},\mathrm{cont}}(EJ\pi) = T^{(1,2)}_{\mathrm{abs},\mathrm{cont}}(EJ\pi) \times \frac{T_{2,\mathrm{cont}}(EJ\pi)}{T_{1,\mathrm{cont}}(EJ\pi) + T_{2,\mathrm{cont}}(EJ\pi)}, \quad (35)$$

with

$$T^{(1,2)}_{\mathrm{abs}_{(f)},\mathrm{cont}}(EJ\pi) = T_{1,\mathrm{cont}}(EJ\pi). \quad (36)$$

where $T_{1,\mathrm{cont}}(EJ\pi)$ was defined in Eq. (25). The weight $p_w(E)$ rises from 0 for excitation energies close to the bottom of the second well V_2 to 1 for the excitation energy V_d where full damping is supposed to be reached:

$$p_w(E) = \frac{\left(E^2 - V_w^2\right)}{\left(V_d^2 - V_w^2\right)\exp[-(E-V_d)/b_w]}, \quad w = 2, \quad (37)$$

with b_w representing an input parameter which defines the weight's behavior.

3. Transmission through triple-humped continuum barriers

Typical triple-humped barriers feature a low thick first barrier with a deep second (superdeformed) well, plus a high and relatively thin double-humped outer barrier with a shallow third (hyperdeformed) well. The role of the fission channels in continuum is quite different for the triple-humped barriers compared to the double-humped ones for two reasons:

(1) The transmission through discrete barriers is low, therefore the transmission through the barriers in continuum is relatively important even at low excitation energies.

(2) The third well may be shallow, and the condition of full damping for the class-III vibrational states could be reached at higher excitation energies, so that direct transmission could occur not only across the discrete barriers [as considered in Eq. (31)], but also across those in continuum (see the next section).

Formally, in a statistical model where the level densities are $(EJ\pi)$ dependent while the transitional states are $(EKJ\pi)$ dependent, it is not possible to have a unitary treatment of both discrete and continuous channels within the optical model for fission. Therefore, we propose to treat partial absorption for the fission channels in the continuum with the surrogate optical model for fission by adopting the following generic expressions based on the generalization of Eqs. (33)–(36):

$$T^{(h,h')}_{\mathrm{dir},\mathrm{cont}}(EJ\pi) = (1 - p_w(E))T^{(h,h')}_{d_{(0)},\mathrm{cont}}(EJ\pi), \quad (38)$$

$$T^{(w,w')}_{\mathrm{abs},\mathrm{cont}}(EJ\pi) = p_w(E)T^{(w,w')}_{i_{(f)},\mathrm{cont}}(EJ\pi). \quad (39)$$

The particular expressions for the direct $T^{(h,h')}_{d_{(0)},\mathrm{cont}}(EJ\pi)$ and indirect $T^{(w,w')}_{i_{(f)},\mathrm{cont}}(EJ\pi)$ coefficients in the limit of zero and full damping, respectively, are obtained by replacing the corresponding indexes in Eq. (33) for the direct transmission, and in Eqs. (35)–(36) for the indirect transmission. The weighting factor $p_w(E)$ is defined according to Eq. (37) for superdeformed $w = 2$ and hyperdeformed $w = 3$ wells, respectively.

C. Fission probability

If fission is assumed to be a compound nucleus (CN) reaction induced by the projectile p with the incident energy E_{in}, its cross section reads

$$\sigma_{p,f}(E_{\mathrm{in}}) = \sum_{J\pi} \sigma_p^{CN}(E_{\mathrm{in}}J\pi)P_f(E_{\mathrm{in}}J\pi), \quad (40)$$

where $\sigma_p^{CN}(E_{\mathrm{in}}J\pi)$ is the cross section of the compound nucleus formation in a state of spin and parity $J\pi$ associated with the incident channel p, and $P_f(E_{\mathrm{in}}J\pi)$ represents the fission probability of the compound nucleus with the excitation energy $E = E^{CM}_{\mathrm{in}} + S_p$ (S_p stands for the separation energy of the particle p in the compound nucleus). The fission probability is defined in terms of the transmission coefficients as

$$P_f(E_{\mathrm{in}}J\pi) = \frac{T_f(EJ\pi)}{\sum_c T_c(EJ\pi) + T_f(EJ\pi)}, \quad (41)$$

where T_f is the fission coefficient and T_c are the transmission coefficients associated to the competing reaction channels. Width fluctuation corrections were not considered in the above equation.

The fission probability proposed in Ref. [26] for a double-humped fission barrier and adopted in many studies, including Ref. [33], has a more elaborate expression because it includes an energy dependent weight function which simulates the coupling between the states from different wells and an average over class-II states. Neglecting the contribution of the delayed

fission, the fission probability reads

$$P_f(E_{\rm in}J\pi) = \frac{T_{\rm dir}^{(1,2)}(EJ\pi)}{\sum_c T_c(EJ\pi) + T_{\rm dir}^{(1,2)}(EJ\pi)}\left(1-\frac{1}{a}\right)+\frac{1}{a}, \quad (42)$$

with

$$a = \left[1 + b^2 + 2b\coth\left(\frac{T_1(EJ\pi)+T_2(EJ\pi)}{2}\right)\right]^{1/2}, \quad (43)$$

$$b = \frac{\left(T_{\rm dir}^{(1,2)}(EJ\pi)+\sum_c T_c(EJ\pi)\right)[T_1(EJ\pi)+T_2(EJ\pi)]}{T_{\rm abs}^{(1,2)}(EJ\pi)T_2(EJ\pi)}. \quad (44)$$

When using this expression, the decay probabilities for the competing channels have to be modified accordingly, to conserve the compound nucleus cross section. This becomes more problematic when transmission through triple-humped barriers with absorption in all wells is involved. The only difference between the fission probability formulations given by Eqs. (41) and (42) is the hyperbolic cotangent factor in Eq. (43) which has as argument the average value of the transmission coefficients through the individual humps (gamma decay to the isomeric state and delayed fission contribution were not considered in the original proposal). Our extended tests confirmed that the effect of this factor on the fission cross section is visible only for fertile nuclei at excitation energies deep below the barrier where transmission coefficients are very small. For these energies the fission cross section is much more sensitive to the width of the barrier than to its height, and one can easily compensate the neglected weight function by slightly increasing the barrier width (within a few tens of keV).

For these reasons, we replaced the fission probability defined by Eq. (42) with the simplified expression given by Eq. (41), which is typical of any decay probability of the compound nucleus. The fission probability given by Eq. (41) does not require modification of the decay probabilities of competing channels. Therefore, the new fission formalism can be easily implemented in existing statistical model codes. We are aware of the approximations of the present model, but it has a good descriptive power of the experimental data, confirms most of the theoretical predictions regarding the fission barrier, and can be used both for fundamental studies and nuclear data evaluation practice.

III. RESULTS AND DISCUSSIONS

The impact of the optical model for fission is significant at excitation energies below and slightly above the barriers. Therefore, the best way to test it would be by fission induced by photons or by direct transfer reactions. However, we chose to present neutron induced fission cross section calculations as they are very important for applications, there are many good-quality experimental data available, and the population cross sections of the resulting compound fissioning nuclei are much better studied. Four representative cases have been selected: two fertile targets, ^{234}U and ^{238}U, and two fissile targets, ^{235}U and ^{239}Pu, whose compound (fissioning) nuclei are supposed to have triple-humped (^{235}U and ^{236}U) and double-humped (^{239}U and ^{240}Pu) fission barriers, accordingly.

TABLE I. Derived fission barrier parameters (in MeV) for fissioning compound nuclei (CN). Values in parentheses correspond to RIPL-3 [47] estimates for double-humped barriers.

CN	V_{h_1}	V_{w_2}	V_{h_2}	V_{w_3}	V_{h_3}	S_n
^{240}Pu	5.97 (6.05)	2.00	5.30 (5.15)			6.53
^{239}U	6.39 (6.45)	2.21	5.82 (6.00)			4.80
^{236}U	4.60	1.60	5.90	4.90	5.64	6.54
^{235}U	4.80	1.60	6.10	5.30	5.78	5.29

The calculations in the fast energy region of the first fission chance (up to $E_n \sim 5$ MeV) are performed with the code EMPIRE 3.2 MALTA [31,49]. The direct cross sections and the particle transmission coefficients are calculated with the ECIS [50] code incorporated into the EMPIRE system using a dispersive optical model potential RIPL 2408 [51,52]. Pre-equilibrium emission at those incident energies is a minor effect. It has been considered by a one-component exciton model with gamma, nucleon, and cluster emissions. The compound nucleus mechanism is described by Hauser-Feshbach [53] and Hoffmann-Richert-Tepel-Weidenmüller (HRTW) [54] statistical models which account for the multiple-particle emission, width fluctuation corrections, and the full gamma cascade. The enhanced generalized superfluid model (EGSM) is employed for the level densities both at equilibrium deformation and at saddle points [47]. The E1 γ-strength function is computed using the modified Lorentzian model (MLO1) [47]. With these models and using recommended parameters retrieved from RIPL-3 [47] or from EMPIRES's internal systematics [31,49] a fair description of the available experimental data have been obtained for the total, elastic, inelastic, and capture cross sections in the studied energy range. More details and complete information about all calculated reaction channels will be given elsewhere, the focus in this paper being on the fission formalism.

The derived humps' and wells' energies of the fundamental fission barriers for fissioning nuclei ^{240}Pu, ^{239}U, ^{236}U, and ^{235}U are given in Table I together with the corresponding neutron separation energies, as needed for the subsequent discussion. These barrier parameters and those defining the transitional states, the class-II/III states, and the level densities at saddles are obtained from the analysis of the fission experimental data, the microscopic predictions, and the empirical systematics as briefly discussed below.

For the fertile targets ^{234,238}U the experimental neutron induced fission cross sections from EXFOR [3] were the most reliable source of information in establishing the starting values for the fission parameters. As shown below for each nucleus, the fission threshold, the slope below the threshold, the absolute value on the plateau, and the presence of resonance structure below and/or above the threshold suggested the shape of the barrier (double or triple humped), the height of the highest hump, the depth of the wells, the energies of the class II (III) states, etc. Other data such as the lifetime of the isomeric

state(s) or the moments of inertia associated with the wells proved to be also very useful as complementary information.

For the fissile targets ^{239}Pu and ^{235}U, the experimental fission cross sections do not provide as much information, therefore the starting values for the fission parameters were extracted from the empirical systematics (mainly for the ^{240}Pu double-humped barrier) and from microscopic calculations (mainly for the ^{236}U triple-humped barrier).

For all studied nuclei, the final values for the fission parameters have been deduced by fitting the experimental cross sections. The double-humped fission barriers for ^{240}Pu and ^{239}U fissioning nuclei are in good agreement with the empirical values tabulated in RIPL-3 that were proposed by Maslov [47], as well as with those proposed by Vladuca and collaborators [55–57]. The fission barriers deduced for ^{240}Pu fissioning nucleus are also in excellent agreement with those obtained by Britt from the analysis of fission isomers [58].

It is presently accepted that there is no unique set of models and parameters which can describe accurately the experimental reaction data, especially the fission cross section. A consistent and reliable set of fission parameters as model independent as possible is the one which provides simultaneously a reasonable description of multiple fission chances induced by neutrons, photons, protons, or direct transfer reactions leading to the same fissionable nucleus. The maximum deviation of the fission parameters needed to describe accurately each type of data may be considered the uncertainty of the corresponding fission parameter. From this type of studies we conclude that the uncertainties of the extrema of a multi-humped fission barrier are around 5%. For a typical barrier height of 6 MeV, that gives about 300 keV of uncertainty, which is still lower than the mass uncertainty estimated in microscopic calculations (e.g., a 500 keV uncertainty of the calculated Hartree-Fock-Bogoliubov masses is estimated in Ref. [59]). However, for a given fissioning nucleus populated in a given reaction with all the other parameters fixed, correlated changes of the extrema of the barrier should be less than 100–150 keV, otherwise the calculated fission cross sections disagree with experimental data.

The measured fission cross section for ^{239}Pu(n,f) and ^{238}U(n,f) reactions retrieved from EXFOR [3] are shown in Figs. 3 and 4. The experimental ^{239}Pu(n,f) cross section is rather smooth in the studied energy range with no vibrational resonances, indicating a full damping of the class-II vibrational states. The ^{238}U(n,f) cross section has a resonant structure only below the fission threshold ($E_n \sim 1.4$ MeV), which is typical for transmission through a double-humped barrier and partially damped class-II vibrational states. In an even-even nucleus such as ^{240}Pu the degree of damping is expected to be lower than in an odd nucleus such as ^{239}U for the same excitation energy in the secondary well. The different degrees of damping suggested by the experimental data are explained by the difference in the neutron separation energies, hence in the different excitation energies in the secondary wells of the two nuclei.

The fission cross section calculation results for ^{239}Pu(n,f) and ^{238}U(n,f) reactions are compared with experimental data

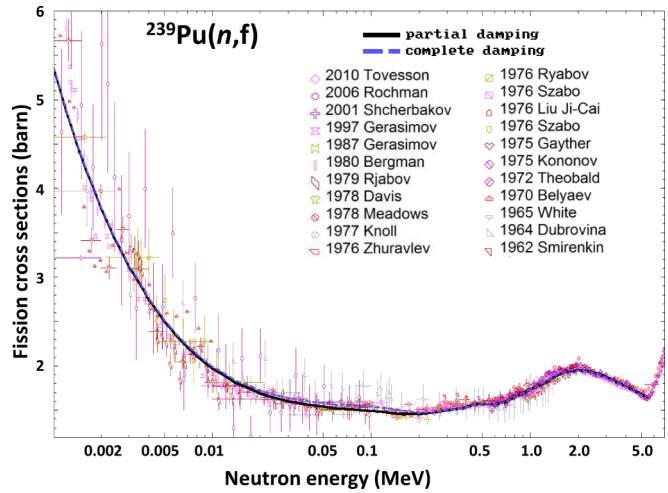

FIG. 3. ^{239}Pu(n,f) cross section calculated considering different degrees of damping for class-II vibrational states: partial damping (full line) and full damping (dotted line). Experimental data are taken from EXFOR [3].

in the same figures. Both partial damping [Eq. (13), solid line] and full damping [Eq. (1), dashed line] assumptions have been used in those calculations. The model calculations support the interpretation given above of the experimental data. For ^{239}Pu(n,f) the solid and dashed curves in Fig. 3 are practically identical, showing that the complete damping limit can be used. This is true for most of the fissile targets with neutron number $N > 146$. For ^{238}U(n,f) the solid curve in Fig. 4 describes the subthreshold resonances, while the dashed curve averages them. Partially damped vibrational resonances are clearly seen below the fission threshold.

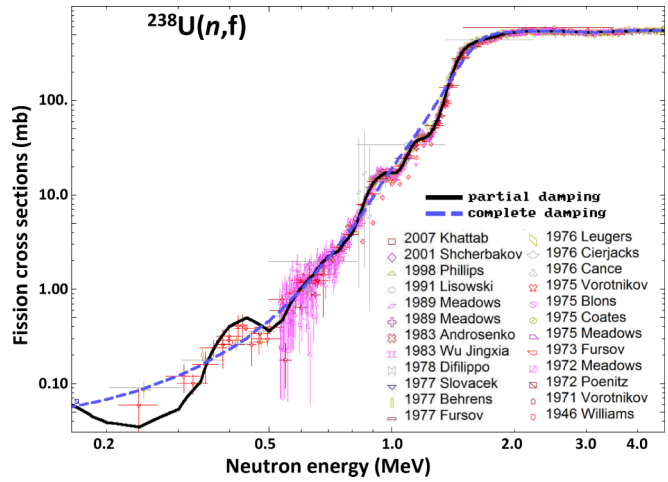

FIG. 4. ^{238}U(n,f) cross section calculated considering different degrees of damping for class-II vibrational states: partial damping (full line) and full damping (dotted line). Experimental data are taken from EXFOR [3].

A third shallow hyperdeformed (HD) minimum in the potential energy of light actinides was predicted more than 40 years ago by Möller *et al.* [60–62] to explain the so called "thorium" anomaly, and it was experimentally confirmed (e.g., see Refs. [63–69]). However, deeper HD minima were found in some works [63–69]. Our own reaction modeling of Ref. [33] supported a shallow depth of the HD minimum for both ^{232}Th and ^{231}Pa targets. Recent theoretical calculations [70–72] confirmed that light uranium and thorium isotopes (among even-Z nuclei) appear to be the best candidates for triple-humped fission barriers with shallow HD minima. This theoretical prediction is also supported by the experimental data on fission cross sections in neutron induced reactions. For example, the experimental ^{234}U(n,f) cross section reveals a resonance structure below and above the threshold ($E_n \sim$ 0.8 MeV) as shown in Fig. 5. The fact that there is no change of slope of the fission cross section below the threshold (which is present for example in ^{233}Th and ^{232}Pa cases [33]) indicates that the height of the first hump ($V_1 = 4.8$ MeV) should be lower than the neutron separation energy $S_n = 5.3$ MeV in ^{235}U; therefore, the class-II vibrational states are completely damped.

The resonance energies with respect to the fission threshold suggest that the difference between the highest hump and the third well is several hundred keV, confirming the hypothesis of triple-humped fission barriers with a shallow third well. As a result, the transmission across the intermediary and the outer barriers in the lower part of the continuum have also a direct component. In other words, the flux reaching the third well through fission channels in the lower part of continuum is not fully absorbed. Therefore, we have to use for the discrete fission channels the transmission coefficients defined in Sec. II B 1 within the optical model for fission, and the partial absorption for the fission channels in the continuum above the outer barrier should be treated with the surrogate optical model for fission described in Sec. II B 3.

The fission cross section calculated considering a full damping of class-II states (full absorption in the secondary well) and different degrees of damping of the class-III vibrational states (partial absorption for discrete channels and for those in lower part of continuum, and partial absorption only for the discrete channels and total absorption for those in continuum) is compared with selected experimental data in Fig. 5.

As mentioned before, there is no unique set of models and parameters which can describe accurately the fission cross section. The ^{235}U(n,f) cross section has been typically modeled using a double-humped fission barrier with parameters chosen to reproduce measured data [47] and Eq. (1) for the fission transmission coefficient. The main assumption is that the class-II states are completely damped at the excitation energies populated in the compound nucleus. However, according to theory [70], the ^{236}U fissioning nucleus should also have a triple-humped barrier with an even shallower third well than ^{235}U.

For this even-even fissioning nucleus, there are collective excited states along the fission path which fill the pairing gap, whose excitation energies at the outer saddle points could exceed the neutron separation energy, and in the third well could be only partially damped. The degree of damping must be higher than in ^{235}U, therefore the damping is reflected only in a decrease of the fission cross section at low energies and not in a resonance structure. Because the third well is so shallow, partial absorption in the third well is also expected for the fission channels in the lower part of continuum, which more significantly decreases the fission cross section. Following for

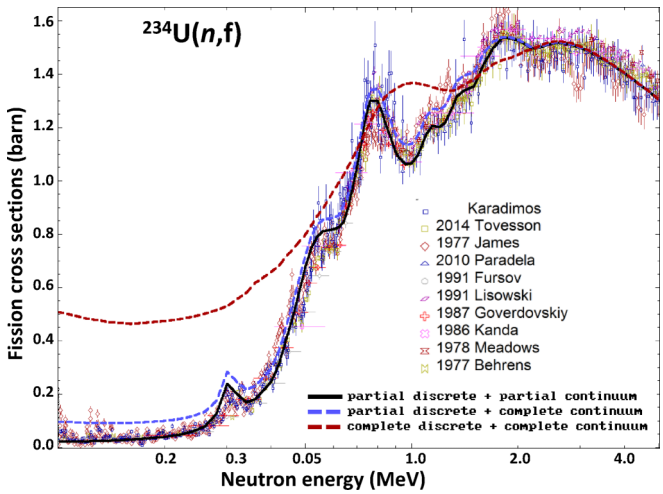

FIG. 5. ^{234}U(n,f) cross section calculated considering complete damping for class-II vibrational states and different degrees of damping for class-III vibrational states associated with partial absorption for discrete and continuum fission channel spectrum (full black line), partial absorption for discrete and full absorption for continuum fission channel spectrum (dashed blue line), and total absorption for discrete and continuum fission channel spectrum (dotted red line). Experimental data are taken from EXFOR [3].

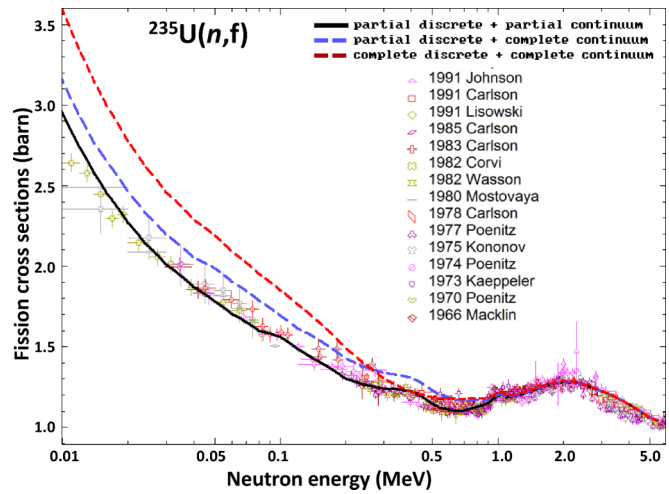

FIG. 6. ^{235}U(n,f) cross section calculated considering full damping for class-II vibrational states and different degrees of damping for class-III vibrational states associated with partial absorption for discrete and continuum fission channel spectrum (full black line), partial absorption for discrete and full absorption for continuum fission channel spectrum (dashed blue line), and total absorption for discrete and continuum fission channel spectrum (dotted red line). Experimental data are taken from EXFOR [3].

^{235}U(n,f) the same procedure used for the ^{234}U(n,f) reaction, the fission cross sections presented in Fig. 6 are obtained. These results show that if the triple-humped barrier is used, then taking into account the partial absorption for all fission channels is mandatory to avoid overestimating the measured fission cross section below 1 MeV of neutron incident energy. The presented ^{235}U(n,f) calculation is, to our knowledge, the first published attempt of using a triple-humped barrier to describe the fission cross section for the ^{235}U(n,f) reaction, which is of utmost importance for nuclear applications.

The results obtained for ^{234,235}U(n,f) cross sections prove that, using a proper fission reaction model and barriers predicted by theory [70], we can achieve a very good agreement with experimental data.

It was mentioned in the Sec. I that the neutron induced fission cross sections of ^{235,238}U are Neutron Standards [4,5], and that the ^{239}Pu(n,f) cross section is a reference cross section fitted within the Neutron Standards project [4,5]. These reference cross sections represent our best (experimental) knowledge. The calculated results of this work agree with neutron reference cross sections of ^{235,238}U(n,f) and ^{239}Pu(n,f) reactions within 3%, which is very important for producing accurate nuclear data evaluations.

IV. CONCLUSIONS

The optical model for fission proposed about 50 years ago has been extended to consider both absorption in wells and partial direct transmission through discrete and continuous fission channels. The corresponding transmission coefficients through multi-humped fission barriers were derived within the JWKB approximation and fission probabilities were defined. The way those fission probabilities are incorporated in the statistical model is comprehensively described. The impact on the calculated fission cross sections of considering partial damping of the vibrational states in the wells, and partial direct transmission through both discrete and continuous fission channels, has been studied. The actual impact depends on the nucleus type, on the incident particle inducing fission, and on the fission barriers' structure. The studied targets have been selected to emphasize the role of the presented formalism in validating and determining the fission barrier parameters, but also in producing accurate, consistent reaction data evaluations. These aspects are of great interest for ongoing international projects such as CIELO [1] and CHANDA [73].

ACKNOWLEDGMENTS

The authors acknowledge Vivian Dimitriou for helpful discussions and provision of some ^{234}U(n,f) experimental data. The work of M.S. was partially supported by the European Commission under ANDES (EURATOM Contract No. FP7-249671) and CHANDA (EURATOM Contract No. FP7-605203).

[1] OECD, Nuclear Energy Agency, Collaborative International Evaluated Library Organisation (CIELO) Pilot Project, WPEC Subgroup 40 (SG40), www.oecd-nea.org/science/wpec/sg40-cielo/.

[2] M. B. Chadwick, E. Dupont, E. Bauge, A. Blokhin, O. Bouland, D. A. Brown, R. Capote, A. Carlson, Y. Danon, C. De Saint Jean, M. Dunn, U. Fischer, R. A. Forrest, S. C. Frankle, T. Fukahori, Z. Ge, S. M. Grimes, G. M. Hale, M. Herman, A. Ignatyuk, M. Ishikawa *et al.*, (The CIELO Collaboration), Neutron reactions on ^{1}H, ^{16}O, ^{56}Fe, ^{235,238}U, and ^{239}Pu, Nucl. Data Sheets **118**, 1 (2014).

[3] N. Otuka, E. Dupont, V. Semkova, B. Pritychenko *et al.*, Towards a more complete and accurate experimental nuclear reaction data library (EXFOR): International collaboration between nuclear reaction data centres (NRDC), Nucl. Data Sheets **120**, 272 (2014), Data available online (e.g., at www-nds.iaea.org/exfor/).

[4] S. Badikov *et al.*, *International Evaluation of Neutron Cross-Section Standards*, Report STI/PUB/1291 (IAEA, Vienna, 2008).

[5] A. D. Carlson, V. G. Pronyaev, D. L. Smith *et al.*, International evaluation of neutron cross section standards, Nucl. Data Sheets **110**, 3215 (2009).

[6] IAEA CIELO Data Development Project, within the International Pilot Project of the OECD/NEA [1], 2014, www-nds.iaea.org/CIELO/.

[7] R. Capote, A. Trkov, M. Sin, M. Herman, A. Daskalakis, and Y. Danon, Physics of neutron interactions with ^{238}U: New developments and challenges, Nucl. Data Sheets **118**, 26 (2014).

[8] R. Capote, A. Trkov, M. Sin, M. W. Herman, and E. Sh. Soukhovitskii, Elastic and inelastic scattering of neutrons on ^{238}U nucleus, EPJ Web Conf. **469**, 00008 (2014).

[9] O. Hahn and F. Strassmann, Über den Nachweis und das Verhalten der bei der Bestrahlung des Urans mittels Neutronen entstehenden Erdalkalimetalle, Naturwiss. **27**, 11 (1939).

[10] L. Meitner and O. R. Frisch, Disintegration of uranium by neutrons: A new type of nuclear reaction, Nature (London) **143**, 239 (1939).

[11] S. Goriely, S. Hilaire, A. J. Koning, M. Sin, and R. Capote, Towards a prediction of fission cross sections on the basis of microscopic nuclear inputs, Phys. Rev. C **79**, 024612 (2009).

[12] S. Bjørnholm and J. E. Lynn, The double-humped fission barrier, Rev. Mod. Phys. **52**, 725 (1980).

[13] O. Bouland, J. E. Lynn, and P. Talou, *R*-matrix analysis and prediction of low-energy neutron-induced fission cross sections over a suite of Pu Isotopes, Phys. Rev. C **88**, 054612 (2013).

[14] J. E. Lynn, Interpretation of neutron-induced fission cross sections and related data, in *First IAEA Symposium on Nuclear Data for Reactors*, Paris, 17–21 October 1966, Report STI/PUB/140, Vol. II (IAEA, Vienna, 1967), pp. 89–114.

[15] P. E. Hodgson, *The Optical Model of Elastic Scattering* (Clarendon Press, Oxford, 1963).

[16] V. M. Strutinsky, Shell effects in nuclear masses and deformation energies, Nucl. Phys. A **95**, 420 (1967).

[17] V. M. Strutinsky, Shells in deformed nuclei, Nucl. Phys. A **112**, 1 (1968).

[18] A. Fubini, J. Blons, A. Michaudon, and D. Paya, Short-Range Intermediate Structure Observed in the ^{237}Np Neutron

Subthreshold Fission Cross Section, Phys. Rev. Lett. **20**, 1373 (1968).
[19] E. Migneco and J. P. Theobald, Resonance grouping structure in neutron induced subthreshold fission of ^{240}Pu, Nucl. Phys. A **112**, 603 (1968).
[20] J. E. Lynn, Structure effects in nuclear fission, in *IAEA Symposium on Nuclear Structure*, Dubna, 4–11 July 1968, Report STI/PUB/189 (IAEA, Vienna, 1968), pp. 463–488.
[21] *Second IAEA Symposium on Physics and Chemistry of Fission*, Vienna, 28 July–21 August 1969, Report STI/PUB/234 (IAEA, Vienna, 1969).
[22] B. B. Back, J. P. Bondorf, G. A. Otroschenko, J. Pedersen, and B. Rasmussen, Analysis of resonances observed in (d,pf)-reactions, in *Second IAEA Symposium on Physics and Chemistry of Fission*, Vienna, 28 July–21 August 1969, Report STI/PUB/234 (IAEA, Vienna, 1969), pp. 351–362.
[23] J. P. Bondorf, Damping effects in the transmission through the double-humped fission barrier, Phys. Lett. B **31**, 1 (1970).
[24] J. E. Lynn and B. B. Back, Sub-barrier fission probability for a double-humped barrier, J. Phys. A: Math. Nucl. Gen. **7**, 395 (1974).
[25] B. B. Back, J. P. Bondorf, G. A. Otroschenko, J. Pedersen, and B. Rasmussen, Fission of U, Np, Pu and Am isotopes excited in the (d, p) reaction, Nucl. Phys. A **165**, 449 (1971).
[26] B. B. Back, O. Hansen, H. C. Britt, and J. D. Garrett, Fission of doubly even actinide nuclei induced by direct reactions, Phys. Rev. C **9**, 1924 (1974).
[27] B. B. Back, H. C. Britt, Ole Hansen, and B. Leroux, Fission of odd-A and doubly odd actinide nuclei induced by direct reactions, Phys. Rev. C **10**, 1948 (1974).
[28] *Third IAEA Symposium on Physics and Chemistry of Fission*, Rochester, New York, 13–17 August 1973, Report STI/PUB/347, Vol. I (IAEA, Vienna, 1974).
[29] A. J. Plompen, T. Kawano, and R. Capote Noy, *Inelastic Scattering and Capture Cross-Section Data of Major Actinides in the Fast Neutron Region*, Technical Report INDC(NDS)-0597 (IAEA, Vienna, 2012).
[30] M. Sin and G. Vladuca, in *Proceedings of the International Conference on Nuclear Data for Science and Technology*, Trieste, Italy, 18–24 May 1997, edited by G. Reffo (Societa Italiana di Fisica, Bologna, 1997), p. 97.
[31] M. Herman, R. Capote, B. V. Carlson, P. Oblozinský, M. Sin, A. Trkov, H. Wienke, and V. Zerkin, Nucl. Data Sheets **108**, 2655 (2007).
[32] B. S. Bhandari, Three-hump fission barrier in ^{232}Th, Phys. Rev. C **19**, 1820 (1979).
[33] M. Sin, R. Capote, A. Ventura, M. Herman, and P. Oblozinský, Fission of light actinides: ^{232}Th(n,f) and ^{231}Pa(n,f) reactions, Phys. Rev. C **74**, 014608 (2006).
[34] R. Capote, L. Leal, Liu Ping, Liu Tingjin, P. Schillebeeckx, M. Sin, I. Sirakov, A. Trkov, and A. L. Nichols, *Evaluated Nuclear Data for Nuclides within the Thorium-Uranium Fuel Cycle*, Report STI/PUB/1435 (IAEA, Vienna, 2011).
[35] M. B. Chadwick, P. Oblozinský, M. W. Herman *et al.*, ENDF/B-VII.0: Next generation evaluated nuclear data library for nuclear science and technology, Nucl. Data Sheets **107**, 2931 (2006).
[36] M. Sin and R. Capote, Transmission through multi-humped fission barriers with absorption: A recursive approach, Phys. Rev. C **77**, 054601 (2008).
[37] M. Sin, R. Capote, S. Goriely, S. Hilaire, and A. J. Koning, Neutron-induced fission cross section on actinides using microscopic fission energy surfaces, in Proceedings of the International Conference on Nuclear Data for Science and Technology, 22–27 April 2007, Nice, France, edited by O. Bersillon, F. Gunsing, E. Bauge, R. Jacqmin, and S. Leray (EDP Sciences, Les Ulis, France, 2008), pp. 313–316.
[38] N. Fröman and P. O. Fröman, *JWKB Approximation, Contributions to the Theory* (North-Holland, Amsterdam, 1965).
[39] N. Fröman and Ö. Dammert, Tunneling and super-barrier transmission through a system of two real potential barriers, Nucl. Phys. A **147**, 627 (1970).
[40] D. L. Hill and J. A. Wheeler, Wheeler, Nuclear Constitution and the Interpretation of Fission Phenomena, Phys. Rev. **89**, 1102 (1953).
[41] B. S. Bhandari, Penetrability through a three-humped barrier in quasi-classical approximation, Nucl. Phys. A **256**, 271 (1976).
[42] B. S. Bhandari, Subbarrier photofission of ^{238}U, Phys. Rev. C **22**, 606 (1980).
[43] T. Martinelli, E. Menapace, and A. Ventura, An improved JWKB approximation for multiple-humped fission barriers, Lett. Nuovo Cimento **20**, 267 (1977).
[44] B. S. Bhandari and A. S. Al-Kharam, Tunneling through equivalent multihumped fission barriers: Some implications for the actinide nuclei, Phys. Rev. C **39**, 917 (1989).
[45] B. S. Bhandari, Test of the adequacy of using smoothly joined parabolic segments to parametrize the multihumped fission barriers in actinides, Phys. Rev. C **42**, 1443 (1990).
[46] T. Belgya, O. Bersillon, R. Capote, T. Fukahori, G. Zhigang, S. Goriely, M. Herman, A. V. Ignatyuk, S. Kailas, A. Koning, P. Obložinský, V. Plujko, and P. Young, *Handbook for Calculations of Nuclear Reaction Data, Reference Input Parameter Library-2*, Technical Report IAEA-TECDOC-1506 (IAEA, Vienna, 2006).
[47] R. Capote *et al.*, RIPL–Reference Input Parameter Library for calculation of nuclear reactions and nuclear data evaluations, Nucl. Data Sheets **110**, 3107 (2009) (see www-nds.iaea.org/RIPL-3/).
[48] S. Bjørnholm, A. Bohr, and B. R. Mottelson, Role of symmetry of the nuclear shape in rotational contributions to nuclear level densities, in *Third IAEA Symposium on Physics and Chemistry of Fission*, Rochester, New York, 13–17 August 1973, Report STI/PUB/347, Vol. I (IAEA, Vienna, 1974), pp. 367–372.
[49] M. Herman *et al.*, *EMPIRE-3.2 Malta User's Manual*, Report INDC(NDS)-0603 (IAEA, Vienna, 2013). Available online at www-nds.iaea.org/publications/indc/indc-nds-0603.pdf.
[50] J. Raynal, Optical model and coupled-channel calculations in nuclear physics, in *Computing as a Language of Physics*, ICTP International Seminar Course, Trieste, Italy, 1971 (IAEA, Vienna, 1972).
[51] R. Capote, E. Sh. Soukhovitskiĭ, J. M. Quesada, and S. Chiba, Is a global coupled-channel dispersive optical model potential for actinides feasible?, Phys. Rev. C **72**, 064610 (2005) (RIPL 2408 potential).
[52] R. Capote, S. Chiba, E. Sh. Soukhovitskiĭ, J. M. Quesada, and E. Bauge, A. global dispersive coupled-channel optical model potential for actinides, J. Nucl. Sci. Technol. **45**, 333 (2008) (RIPL 2408 potential).
[53] W. Hauser and H. Feshbach, The inelastic scattering of neutrons, Phys. Rev. **87**, 366 (1952).
[54] H. M. Hoffmann, J. Richert, J. W. Tepel, and H. A. Weidenmüller, Direct reactions and Hauser-Feshbach theory, Ann. Phys. (N.Y.) **90**, 403 (1975).

[55] M. Sin, G. Vladuca, and A. Tudora, Subbarrier fission probabilities of ^{240}Pu, Ann. Nucl. Energy **24**, 1027 (1997).

[56] G. Vladuca, M. Sin, and A. Tudora, Neutron cross sections of ^{239}Pu in the energy range 0.01–6 MeV, Ann. Nucl. Energy **24**, 1127 (1997)

[57] G. Vladuca, M. Sin, and C. C. Negoita, Neutron cross sections of ^{238}U in the energy range 0.01–5.5 MeV, Ann. Nucl. Energy **27**, 995 (2000)

[58] H. C. Britt, Properties of fission isomers, At. Data Nucl. Data Tables **12**, 407 (1973).

[59] S. Goriely and R. Capote, Uncertainties of mass extrapolations in Hartree-Fock-Bogoliubov mass models, Phys. Rev. C **89**, 054318 (2014).

[60] P. Möller, S. G. Nilsson, and R. K. Sheline, Octupole deformations in the nuclei beyond ^{208}Pb, Phys. Lett. B **40**, 329 (1972).

[61] P. Möller, Odd-multipole shape distortions and the fission barriers of elements in the region $84 \leqslant z \leqslant 120$, Nucl. Phys. A **192**, 529 (1972).

[62] P. Möller and J. R. Nix, Calculation of fission barriers, in *Third IAEA Symposium on Physics and Chemistry of Fission*, Rochester, New York, 13–17 August 1973, Report STI/PUB/347, Vol. I (IAEA, Vienna, 1974), pp. 103–1490.

[63] J. Blons, C. Mazur, and D. Paya, Evidence for Rotational Bands Near the ^{232}Th(n,f) Fission Threshold, Phys. Rev. Lett. **35**, 1749 (1975).

[64] J. Blons, C. Mazur, D. Paya, M. Ribrag, and H. Weigmann, Rotational Bands in Asymmetrically Deformed ^{231}Th, Phys. Rev. Lett. **41**, 1282 (1978).

[65] J. Blons, B. Fabbro, C. Mazur, D. Paya, M. Ribrag, and Y. Patin, High resolution fission probabilities for ^{229,230,232}Th(d,pf) and ^{233,236}U(d,pf) reactions, Nucl. Phys. A **477**, 231 (1988).

[66] A. Krasznahorkay, M. Hunyadi, M. N. Harakeh, M. Csatlós, T. Faestermann, A. Gollwitzer, G. Graw, J. Gulyás, D. Habs, R. Hertenberger, H. J. Maier, Z. Máté, D. Rudolph, P. Thirolf, J. Timár, and B. D. Valnion, Experimental Evidence for Hyperdeformed States in U Isotopes, Phys. Rev. Lett. **80**, 2073 (1998).

[67] A. Krasznahorkay, D. Habs, M. Hunyadi, D. Gassmann, M. Csatlós, Y. Eisermann, T. Faestermann, G. Graw, J. Gulyás, R. Hertenberger, H. J. Maier, Z. Máté, A. Metz, J. Ott, P. Thirolf, and S. Y. van der Werf, On the excitation energy of the ground state in the third minimum of ^{234}U, Phys. Lett. B **461**, 15 (1999).

[68] P. G. Thirolf and D. Habs, Spectroscopy in the second and third minimum of actinide nuclei, Prog. Part. Nucl. Phys. **49**, 325 (2002).

[69] M. Csatlós, A. Krasznahorkay, P. G. Thirolf, D. Habs, Y. Eisermann, T. Faestermann, G. Graw, J. Gulyás, M. N. Harakeh, R. Hertenberger, M. Hunyadi, H. J. Maier, Z. Máté, O. Schaile, and H.-F. Wirth, Resonant tunneling through the triple-humped fission barrier of ^{236}U, Phys. Lett. B **615**, 175 (2005).

[70] T. Ichikawa, P. Möller, and A. J. Sierk, Character and prevalence of third minima in actinide fission barriers, Phys. Rev. C **87**, 054326 (2013).

[71] P. Jachimowicz, M. Kowal, and J. Skalski, Eight-dimensional calculations of the third barrier in ^{232}Th, Phys. Rev. C **87**, 044308 (2013).

[72] J. D. McDonnell, W. Nazarewicz, and J. A. Sheikh, Third minima in thorium and uranium isotopes in a self-consistent theory, Phys. Rev. C **87**, 054327 (2013).

[73] European Commission Project 605203: Solving Challenges in Nuclear Data for the Safety of European Nuclear Facilities, funded under FP7-EURATOM-FISSION, www.chanda-nd.eu/.